Nuclear magnetic resonance on oriented 4.7 h $^{99}Rh^m$, 4.3 d $^{101}Rh^m$, and 2.9 d ^{97}Ru after recoil implantation into Fe

R. Eder, E. Hagn, and E. Zech
Physik-Department, Technische Universität München, D-8046 Garching, Federal Republic of Germany
(Received 9 July 1985)

The magnetic hyperfine splitting frequencies $\nu_M = |g\mu_N B_{HF}/h|$ of $^{99}Rh^m$ ($T_{1/2}=4.7$ h; $I^\pi=\frac{9}{2}^+$) and $^{101}Rh^m$ ($T_{1/2}=4.3$ d; $I^\pi=\frac{9}{2}^+$) in Fe were measured with nuclear magnetic resonance on oriented nuclei as 534.28(5) MHz and 516.10(5) MHz, respectively. With the hyperfine field $B_{HF}(RhFe)=-556.6(1.2)$ kG the g factors are deduced to be $^{99}Rh^m$: $|g|=1.2595(27)$; $^{101}Rh^m$: $|g|=1.2167(26)$. The g factors are discussed in the framework of the systematics of $\pi g_{9/2}$ states. The new data give strong evidence that the $\frac{7}{2}^+$ states appearing in Rh at rather low excitation energies cannot be described by a $|(\pi g_{9/2})^3\rangle_{7/2^+}$ configuration as adopted up to now. In addition, the hyperfine splitting frequency of ^{97}Ru in Fe was remeasured to be 117.58(2) MHz. With the hyperfine field $B_{HF}(RuFe)=-489.6(4.0)$ kG, the g factor of $\frac{5}{2}^+$ ^{97}Ru is determined to be $|g|=0.315(3)$. The resonance shifts of ^{52}Mn, ^{97}Ru, $^{99}Rh^m$, and $^{101}Rh^m$ in Fe were measured in external magnetic fields up to 10 kG. The relative Knight shifts are discussed.

I. INTRODUCTION

In the odd Rh isotopes the energetically lowest single-particle states arise from the $\pi g_{9/2}$ and $\pi p_{1/2}$ orbitals. In addition, a low-lying $\frac{7}{2}^+$ state is known, which decreases in energy from 201 keV in ^{99}Rh to 40 keV in ^{103}Rh, and which is the ground state of ^{105}Rh.[1] This state, which cannot be explained by a single-particle configuration, has been interpreted as a three-quasiparticle intruder state (configuration $|(\pi g_{9/2})^3\rangle_{7/2^+}$).[2,3] This assignment can be tested by measurements of the nuclear g factor, as for this configuration $g(\frac{7}{2}^+)=g(\pi g_{9/2})$ is expected. Kempter and Klein[4] reported a nuclear magnetic resonance on oriented nuclei (NMR-ON) measurement on $\frac{7}{2}^+$ $^{103}Rh^m$ in Fe; assuming $K=0$ for the Knight shift of $RhFe$, they deduced $g=1.224(22)$, which was regarded to fit fairly well into the systematics of neighboring $\frac{9}{2}^+$ states, thus supporting the three-quasiparticle structure of the $\frac{7}{2}^+$ state. Although they derived a second value for the g factor from the zero-field hyperfine splitting, $g=1.290(7)$, they did not discuss the fact that this value would contradict the three-quasiparticle structure of the $\frac{7}{2}^+$ state. Hagn *et al.*[5] reported NMR-ON measurements on $\frac{7}{2}^+$ ^{105}Rh in Fe and Ni. They deduced a g factor of 1.272(2), which did not fit into the known systematics of $\frac{9}{2}^+$ states. Because of some uncertainties in the hyperfine field due to (experimentally unknown) hyperfine anomalies, Hagn *et al.* did not draw final conclusions concerning the structure of the $\frac{7}{2}^+$ state.

Here we report NMR-ON measurements on $\frac{9}{2}^+$ $^{99}Rh^m$ and $^{101}Rh^m$ in Fe. As the hyperfine anomalies between the $\frac{7}{2}^+$ and $\frac{9}{2}^+$ states are expected to be small, ratios of g factors of $\frac{9}{2}^+$ $^{99}Rh^m$ and $^{101}Rh^m$ and $\frac{7}{2}^+$ $^{103}Rh^m$ and ^{105}Rh can now be deduced with high accuracy, independent of the exact knowledge of the hyperfine field. The trend of g factors deduced in the present work contradicts the three-quasiparticle structure of the $\frac{7}{2}^+$ states.

In addition, we redetermined the magnetic moment of ^{97}Ru, and measured the resonance shifts of ^{52}Mn, ^{97}Ru, and $^{99,101}Rh^m$ in the same Fe sample, from which relative Knight shifts were determined.

II. EXPERIMENTAL PROCEDURE

A. Nuclear orientation (NO) and nuclear magnetic resonance on oriented nuclei (NMR-ON)

The angular distribution of γ rays emitted in the decay of oriented nuclei is given by[6]

$$W(\theta,T)=1+\sum_{k=2,4} B_k^{(I)} A_k P_k(\cos\theta) Q_k \ . \tag{1}$$

Here the parameters A_k are products of the normally used angular correlation coefficients U_k and F_k, which depend on the spins and multipolarities of the decay cascade. Tabulated values are given in Ref. 7. The $P_k(\cos\theta)$ are Legendre polynomials, θ being the angle between the quantization axis—here the external magnetic field—and the direction of observation, and Q_k are solid angle correction coefficients. The $B_k^{(I)}$ describe the degree of orientation; in the present case of "magnetic NO" they depend on the spin I and on $h\nu_M/k_BT$, where T is the temperature of the system and ν_M is the magnetic hyperfine splitting frequency,

$$\nu_M = |g\mu_N B_{HF}/h| \ . \tag{2}$$

Here g is the nuclear g factor and B_{HF} is the magnetic hyperfine field. For the validity of Eq. (1) it has tacitly been assumed that 100% of the impurity nuclei are subject to one unique hyperfine field, which is not necessarily

fulfilled in practice. In many cases it is a good approximation to assume that a fraction f of the nuclei is subject to the full undisturbed hyperfine field, while the residual nuclei with a fraction of $1-f$ are on lattice sites with a negligibly small hyperfine interaction. For this case Eq. (1) reduces to

$$W(\theta,T)=1+f\sum_{k=2,4}B_k^{(I)}A_kP_k(\cos\theta)Q_k\ . \tag{3}$$

From simultaneous measurements of $W(0°,T)$ and $W(90°,T)$, ν_M, fA_2, and fA_4 can be determined with least-squares fits without any assumptions about the decay cascade. The full-field fraction f can then be determined via the anisotropy of a transition for which all decay parameters are known. With the knowledge of f, decay parameters such as spins, γ multipolarities, and multipole mixing ratios are obtained for all observed γ transitions.

In the NMR-ON method,[8] a rf-induced change of the sublevel populations is detected via the corresponding change of the radiation pattern of the γ rays. The resonance condition is given by

$$\nu=\nu_M+|g\mu_N/h|\,\mathrm{sgn}(B_{HF})(1+K)B_0\ , \tag{4}$$

where $\mathrm{sgn}(B_{HF})$ is the sign of the hyperfine field with respect to the external magnetic field B_0, and K is a parameter including the Knight shift and diamagnetic shielding.

B. The decay scheme

A simplified decay scheme of 4.7 h $^{99}Rh^m$ according to Ref. 1 is shown in Fig. 1. The up to now unknown spin of the 1261 keV level is determined in this work via the anisotropy of the 1261 keV transition to be $\frac{7}{2}$.

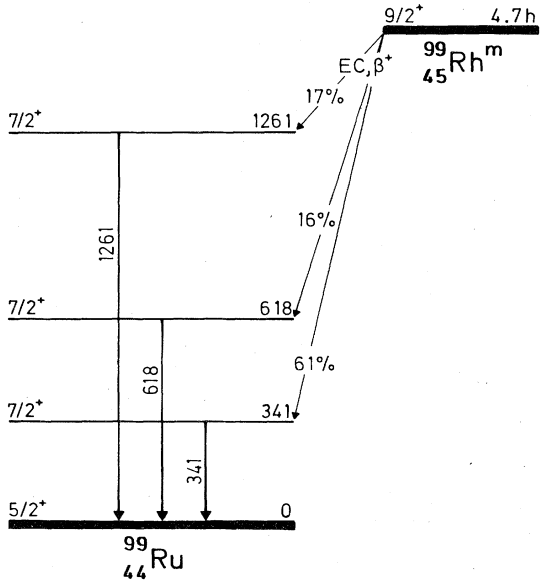

FIG. 1. Simplified decay scheme of $^{99}Rh^m$.

III. EXPERIMENTAL DETAILS

The $^{99}Rh^mFe$ sample was prepared by the recoil implantation technique.[9] A target stack consisting of 12 ^{102}Pd foils (isotopic enrichment 77.9%, thickness 1.0 mg/cm^2) and 12 Fe foils (thickness 1.5 mg/cm^2; purity $\geq$99.999%) in alternating order was irradiated at the cyclotron in Karlsruhe for 4 h with 100 MeV alpha particles (average current 3 μA). $^{99}Rh^m$ is produced via the compound reactions $^{102}Pd(\alpha,xnyp)$ with $x+y=7$. All produced $A=99$ isotopes feed $^{99}Rh^m$ via the decay chain

$$^{99}Cd\rightarrow{}^{99}Ag\rightarrow{}^{99}Pd\rightarrow{}^{99}Rh^m\ .$$

The recoil distance of the $A=99$ isotopes with a kinetic energy of 4 MeV is $\sim$0.3 μm. Thus all nuclei which are produced in the rear surface layers with a thickness of $\sim$0.3 μm are implanted homogeneously into the Fe foils. In addition, the following isotopes were observed in the Fe foils:

^{97}Ru ($T_{1/2}=2.9$ d);

^{100}Pd ($T_{1/2}=3.7$ d);

^{101}Pd ($T_{1/2}=8.5$ h);

^{100}Rh ($T_{1/2}=20$ h);

$^{101}Rh^m$ ($T_{1/2}=4.4$ d);

^{52}Mn ($T_{1/2}=5.7$ d).

As the hyperfine splitting frequency of ^{52}Mn in Fe is known experimentally, the respective γ anisotropy can be used for thermometry. After the irradiation the most active parts of the Fe foils were soldered to the Cu cold finger of an adiabatic demagnetization cryostat and cooled to $\sim$10 mK. The γ rays were detected with two coaxial Ge(Li) detectors which were placed at 0° and 90° with respect to the external polarizing field B_0. The rf field was applied perpendicular to B_0 with a one-turn rf coil. A voltage-controlled rf generator was used (Rohde and Schwarz, type SMLU). The center frequency is continuously regulated by a feed-back system which compares the nominal frequency with the actual center frequency measured with a repetition rate of 300 Hz by a high-precision frequency counter. As the FM modulation frequency is synchronized with the frequency counter, the actual center frequency is used for the feed-back system, independent of the modulation band width. Details of the cryostat and the electronic equipment are described elsewhere.[10] Here we only want to mention that always an even number of NMR-ON spectra were added, in order to avoid spurious shifts of the resonance centers in "sweep-direction" introduced by the finite spin-lattice relaxation time. (See, e.g., the discussion in Ref. 11.)

IV. RESULTS

A. NMR-ON experiments

The NMR-ON resonance of $^{99}Rh^m$ was searched in the following way: Starting at 500 MHz, the rf frequency,

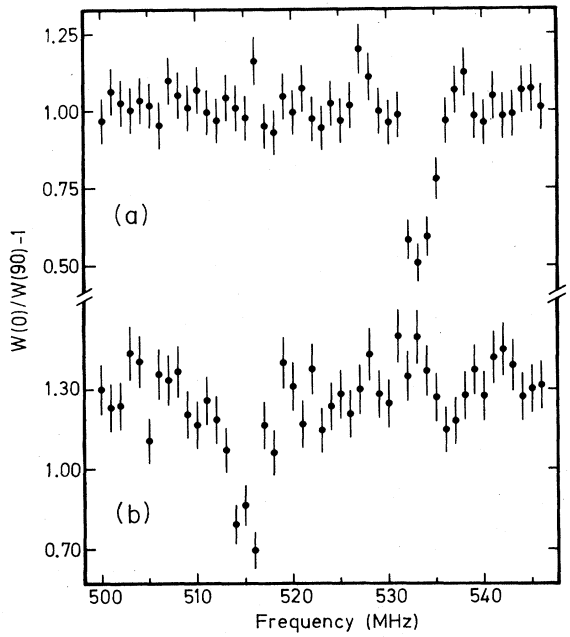

FIG. 2. Resonance search: γ anisotropies of the 341 keV transition of $^{99}Rh^m$ (a) and the 307 keV transition of $^{101}Rh^m$ (b) vs frequency. The NMR-ON of both isotopes in Fe are well observable. External magnetic field $B_0=0.96(2)$ kG. Total counting time ~ 1 h.

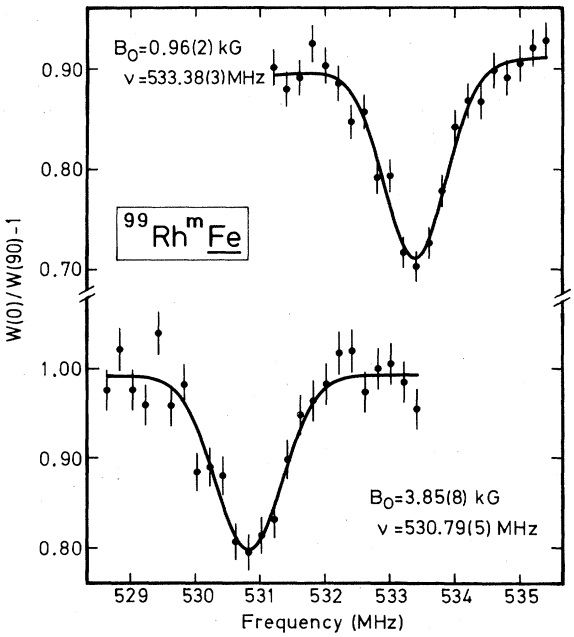

FIG. 3. NMR-ON resonances of the 341 keV transition of $^{99}Rh^m$ measured for two different external magnetic fields.

which was FM modulated with 1 kHz and a total modulation band width of 2 MHz, was increased every 100 s in 1 MHz steps. Figure 2 shows the γ anisotropy of the 341 keV transition of $^{99}Rh^m$ (top) and the 307 keV transition of $^{101}Rh^m$ (bottom). The NMR-ON resonances were found at ~ 533 and ~ 515 MHz for $^{99}Rh^m$ and $^{101}Rh^m$, respectively. All further measurements were performed in reduced frequency regions adjusted to the respective isotope.

1. $^{99}Rh^mFe$

Figure 3 shows two NMR-ON resonances of $^{99}Rh^mFe$ measured in external magnetic fields $B_0=0.96(2)$ and 3.85(8) kG. Further measurements were performed for $B_0=1.92(4)$ and 5.77(12) kG. The observed line widths are listed in Table I. The slight increase of the line widths with increasing B_0 is probably due to the increase of the spin-lattice relaxation time with B_0, as discussed, e.g., in detail in Ref. 12. It should be pointed out, however, that the line widths, which are in ferromagnetic samples always dominated by inhomogeneous broadening, are rather small. The resonance centers vs B_0 are illustrated in Fig. 4. The least-squares fit yields

$$\nu(B_0=0)=534.28(5)\ \text{MHz}\ ,$$

$$d\nu/dB_0=-0.914(20)\ \text{MHz/kG}\ .$$

2. $^{101}Rh^mFe$

Figure 5 shows two NMR-ON spectra of the 307 keV transition of $^{101}Rh^mFe$ measured in external magnetic fields $B_0=0.96(2)$ and 3.85(8) kG. Further measurements were performed for $B_0=1.92(4)$, 5.77(12), 7.69(15), and 10.6(2) kG. The observed line widths are listed in Table I.

TABLE I. Observed resonance line widths.

	Γ (MHz)			
B_0 (kG)	$^{99}Rh^mFe$[a]	$^{101}Rh^mFe$[b]	$^{97}RuFe$[c]	$^{52}MnFe$[b]
0.96(2)	1.12(9)	0.99(5)	0.26(2)	0.54(7)
1.92(4)	1.12(11)	1.14(8)		0.49(5)
3.85(8)	1.22(13)	1.27(9)	0.30(2)	0.85(17)
5.77(12)	1.46(20)	1.46(9)		0.61(12)
6.73(13)			0.36(2)	
7.69(15)		1.46(7)		0.74(12)
10.6(2)		1.64(12)	0.44(3)	0.69(14)

[a]Including the total modulation band width of 0.6 MHz.
[b]Including the total modulation band width of 0.3 MHz.
[c]Including the total modulation band width of 0.1 MHz.

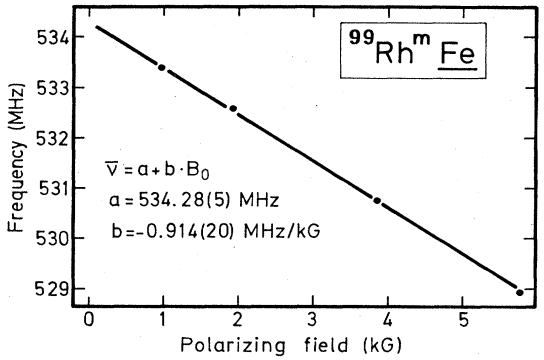

FIG. 4. Shift of the $^{99}Rh^{m}Fe$ NMR-ON resonance with the external magnetic field.

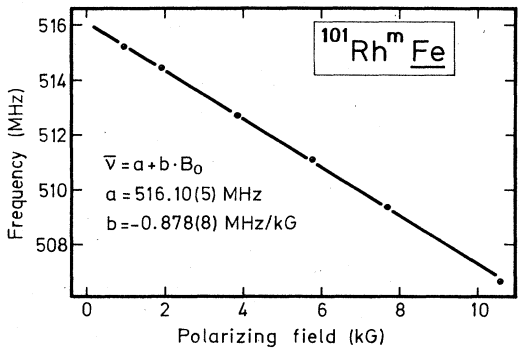

FIG. 6. Shift of the $^{101}Rh^{m}Fe$ NMR-ON resonance with the external magnetic field.

Again a slight increase of the line widths with B_0 is observed. The resonance amplitude drops from ~ 0.3 at 0.96 kG to ~ 0.12 at 10.6 kG, most probably because of the decreasing enhancement factor for the rf field. The resonance centers vs B_0 are illustrated in Fig. 6. The final results are

$$\nu(B_0=0)=516.10(5)\ \text{MHz}\ ,$$

$$d\nu/dB_0=-0.878(8)\ \text{MHz/kG}\ .$$

3. $^{97}RuFe$

Figure 7 shows a NMR-ON spectrum of the 215 keV transition of $^{97}RuFe$ measured in an external magnetic field $B_0=0.96(2)$ kG. Further measurements were performed for $B_0=3.85(8)$, 6.73(13), and 10.6(2) kG. The observed line widths are listed in Table I. These line widths are considerably smaller than $\Gamma=1.2$–1.6 MHz obtained by Leuthold *et al.*[11] In their experiments a sample was used which was prepared by neutron irradiation, and which contained the relatively high Ru concentration of 1 at. %. The resonance centers vs B_0 are illustrated in Fig. 8. The final results are

$$\nu(B_0=0)=117.58(2)\ \text{MHz}\ ,$$

$$d\nu/dB_0=-0.234(2)\ \text{MHz/kG}\ .$$

The hyperfine splitting and the resonance shift are slightly different from 117.69(2) MHz and $-0.246(3)$ MHz/kG, respectively, of Ref. 11. The difference of the hyperfine splitting is most probably due to a (slight) dependence of the hyperfine field on the Ru impurity concentration. A similar effect has, e.g., been observed for Au in Fe.[13] The difference of the resonance shift is in our opinion connected with the relatively large line width of Ref. 11: Because of the high Ru impurity concentration the lattice is disturbed in the neighborhood of the ^{97}Ru impurities. This implies in our opinion a variation of the spin-lattice relaxation time of ^{97}Ru over the resonance line width. In the nonsaturation region, i.e., especially for the

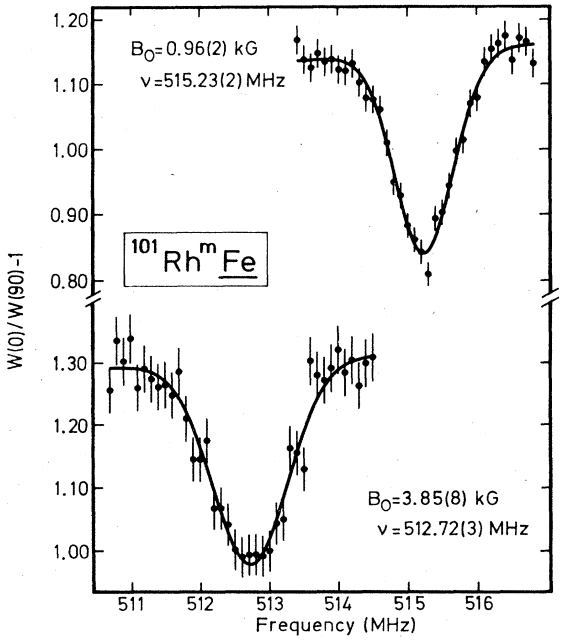

FIG. 5. NMR-ON resonances of the 307 keV transition of $^{101}Rh^{m}$ measured for two different external magnetic fields.

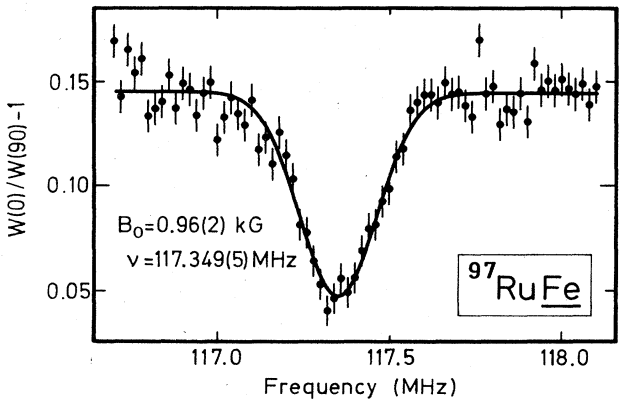

FIG. 7. NMR-ON resonance of the 215 keV transition of ^{97}Ru measured for $B_0=0.96(2)$ kG. Note that the frequency resolution is 20 kHz.

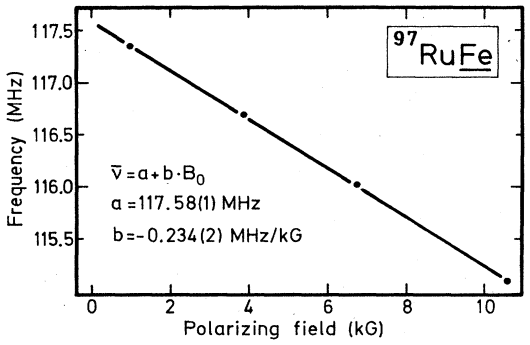

FIG. 8. Shift of the ^{97}Ru*Fe* NMR-ON resonance with the external magnetic field.

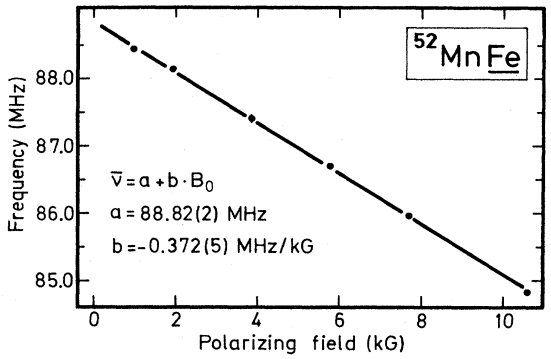

FIG. 10. Shift of the ^{52}Mn*Fe* NMR-ON resonance with the external magnetic field.

larger external magnetic fields, the resonance amplitude depends on the ratio of rf power to the spin-lattice relaxation matrix element, which can vary with the frequency over the resonance line width. In this way, a spurious shift of the effective resonance centers with B_0 may be introduced, leading to (slightly) different resonance shifts. This does not apply to the present case because of the extremely small impurity concentrations. Systematic investigations of the spin-lattice relaxation matrix element and the dependence on the external magnetic field over the inhomogeneously broadened resonance line widths are in progress.

4. ^{52}MnFe

Figure 9 shows a NMR-ON spectrum of the 1434 keV transition of ^{52}Mn*Fe* measured in an external magnetic field $B_0 = 0.96(2)$ kG. Further measurements were performed for $B_0 = 1.92(4)$, 3.85(8), 5.77(12), 7.69(15), and 10.6(2) kG. The observed line widths are listed in Table I. The resonance centers vs B_0 are illustrated in Fig. 10. The final results are

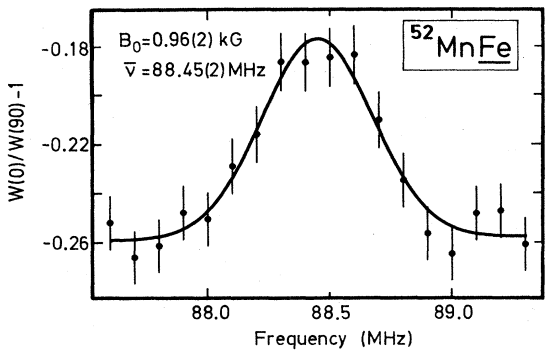

FIG. 9. NMR-ON resonance of the 1434 keV transition of ^{52}Mn measured for $B_0 = 0.96(2)$ kG.

$$\nu(B_0 = 0) = 88.82(2) \text{ MHz} ,$$

$$d\nu/dB_0 = -0.372(5) \text{ MHz/kG} .$$

The hyperfine splitting is slightly different from 88.71(1) MHz of Ref. 14, which in our opinion is due to the different purity of the Fe foils. (In the experiments of Ref. 14 commercially available Fe foils with a nominal purity of 99.9% were used.) The resonance shift, however, is in good agreement with −0.371(7) MHz/kG of Ref. 14.

B. γ anisotropies

γ anisotropies were measured for $B_0 = 5.77(12)$ kG in the temperature region 11—13 mK. Taking into account the known NMR-ON frequencies, fA_2 and fA_4 were determined according to Eq. (3). The results are listed in Table II.

V. DISCUSSION

A. Hyperfine interaction aspects

The presently known hyperfine splitting frequencies of Rh isotopes in Fe and Ni are listed in Table III, together with the respective ratio for ^{101}Rh^m and ^{105}Rh. This ratio, which represents the ratio of the hyperfine fields in Fe and Ni, and which should be independent of the isotope, is slightly different for ^{101}Rh^m and ^{105}Rh. The double ratio

TABLE II. fA_2 and fA_4 of transitions in ^{99}Rh^m, ^{101}Rh^m, and ^{97}Ru.

Isotope	Energy (keV)	fA_2	fA_4
^{99}Rh^m	361	+0.363(10)	+0.05(2)
	1261	+0.40(4)	+0.10(8)
^{101}Rh^m	307	+0.461(8)	−0.29(1)
^{97}Ru	215	+0.46(2)	−0.2(6)

$$[\nu_M(^{101}\mathrm{Rh}^m Fe)/\nu_M(^{101}\mathrm{Rh}^m Ni)]/[\nu_M(^{105}\mathrm{Rh}Fe)/\nu_M(^{105}\mathrm{Rh}Ni)]=0.993(2)$$

is smaller than the nominal value 1.0. This means that one of the four hyperfine splitting frequencies is incorrect. In our opinion one of the following two possibilities yields the most probable explanation:

(1) The hyperfine splitting of $^{101}\mathrm{Rh}^m Ni$ measured by Kaindl *et al.*[15] is too small by 1.5 MHz. This could be due to the different sample preparation technique. Kaindl *et al.* prepared their sample by deuteron irradiation of natural ruthenium, chemical separation and electroplating of the Rh activity onto a nickel foil. It may be possible that impurities are introduced during this long procedure. The resonance line widths are normally enlarged considerably by such impurities. It has been shown experimentally that for large line widths the resonance center does not necessarily represent the dilute-impurity hyperfine interaction.

(2) The $^{105}\mathrm{Rh}Fe$ and $^{105}\mathrm{Rh}Ni$ samples used by Hagn *et al.*[5] were prepared by neutron irradiation of $^{104}\mathrm{Ru}Fe$ and $^{104}\mathrm{Ru}Ni$ alloys, the final Ru concentration being 0.1 at.%. Although the dilute-impurity limit should already be fulfilled at the impurity level of 0.1 at.%, a (small) concentration dependency of the hyperfine field of Rh*Fe* or Rh*Ni* cannot be excluded. Thus further experimental investigations will be necessary to clarify this discrepancy.

The derivation of the hyperfine field of Rh*Fe* has been outlined in detail in Ref. 5. We will use the value

$$B_{\mathrm{HF}}(\mathrm{Rh}Fe)=-556.6(1.2)\ \mathrm{kG}$$

for the determination of the nuclear g factors.

B. Resonance shifts

From the measured resonance shifts K parameters are derived according to Eq. (4), which are listed in Table IV together with data from the literature.[4,5,14] Our new data for $^{99}\mathrm{Rh}^m Fe$ and $^{101}\mathrm{Rh}^m Fe$, $K=-4.8(2.1)\%$ and $-5.3(1.1)\%$, respectively, are in good agreement with $K(^{103}\mathrm{Rh}^m Fe)=-5.6(1.7)\%$ (Ref. 4) and $K(^{105}\mathrm{Rh}Fe)=-4.5(1.3)\%$ (Ref. 5). The $^{52}\mathrm{Mn}Fe$ shift is also in good agreement with the result of Ref. 14. As three independent experiments on Rh isotopes give consistent results, with an average value of $K=-5.1(7)\%$, it seems to be improbable that it originates from a spurious effect. The following possibilities remain for the explanation:

TABLE III. Hyperfine splitting frequencies of Rh isotopes in Fe and Ni.

Isotope	ν_{Fe} (MHz)	ν_{Ni} (MHz)	$\nu_{\mathrm{Fe}}/\nu_{\mathrm{Ni}}$
$^{99}\mathrm{Rh}^m$	534.28(5)[a]		
$^{101}\mathrm{Rh}^m$	516.10(5)[a]	207.1(4)[b]	2.492(5)
$^{103}\mathrm{Rh}^m$	550.3(5)[c]		
$^{105}\mathrm{Rh}$	539.62(3)[d]	218.06(5)	2.4746(6)

[a]This work.
[b]Extrapolated to zero external field. Kaindl *et al.* (Ref. 15) quote 206.2(4) MHz for an external field of 1 kG.
[c]Reference 4.
[d]Reference 5.

(1) The hyperfine field of Rh*Fe* is smaller by 5.1(6)%, yielding in this way to $K=0$. This is highly improbable, as two independent low-temperature measurements exist for the hyperfine field:

$^{100}\mathrm{Rh}(2^+)Fe$: $B_{\mathrm{HF}}=-556.5(1.2)$ kG.[16] As the fractional contribution of the $g_{9/2}$ proton to the magnetic moment is known to be 0.95(5), the hyperfine anomaly between the 2^+ state and the $\frac{9}{2}^+$ or $\frac{7}{2}^+$ states is negligibly small. (The single-level anomalies of these states calculated according to Eisinger and Jaccarino[17] vary between -0.44% and -0.46%.) For a detailed discussion we refer to Ref. 5.

$^{103}\mathrm{Rh}(\frac{1}{2}^-)Fe$: $B_{\mathrm{HF}}=-536.86(12)$ kG. The $\frac{1}{2}^-$ state is expected to have a large single-level hyperfine anomaly. The calculation according to Ref. 17 yields -4.2%. The application of the empirical rule of Moskowitz and Lombardi,[18] which has been based on a theoretical basis by Fujitu and Arima,[19] yields, assuming a Z^2 scaling, -4.1%. In this way the different hyperfine fields between $^{100}\mathrm{Rh}(2^+)$ and $^{103}\mathrm{Rh}(\frac{1}{2}^-)$ in Fe are well understood. Thus the possibility of a wrong hyperfine field can be excluded with high confidence.

(2) There exist nonzero Knight shifts in Fe matrices up to several percent which depend possibly on the type of the impurity-host combination, as had already been pointed out in Ref. 20.

(3) There exists a "hidden" effect, which has not been recognized up to now, which gives rise to an anomalous resonance shift. In the case of Ir*Ni* an anomalously high resonance shift could be explained by the observed fact that the main part of the experimental line width was due to quadrupole interaction, and that the relative amplitudes of the quadrupole subresonances changed with the external magnetic field.[10] To clarify the situation further

TABLE IV. Resonance shifts of Mn, Ru, and Rh isotopes in Fe.

Isotope	$d\nu/dB_0$ (MHz/kG)	K (%)	Ref.
$^{52}\mathrm{Mn}$	$-0.372(5)$	$-4.1(1.5)$	a
	$-0.371(7)$	$-4.7(1.8)$	b
$^{97}\mathrm{Ru}$	$-0.234(2)$	$-2.5(1.3)$	a
$^{99}\mathrm{Rh}^m$	$-0.914(20)$	$-4.8(2.1)$	a
$^{101}\mathrm{Rh}^m$	$-0.878(10)$	$-5.3(1.1)$	a
$^{103}\mathrm{Rh}^m$	$-0.933(17)$	$-5.6(1.7)$	c
$^{105}\mathrm{Rh}$	$-0.926(13)$	$-4.5(1.3)$	d

[a]This work.
[b]Reference 14.
[c]Reference 4.
[d]Reference 5.

NMR-ON experiments with higher external magnetic fields seem to be necessary.

C. Decay parameters

For the interpretation of the measured fA_k coefficients listed in Table II, we have first to determine the full-field fraction f. The known phase diagrams of Ru*Fe* and Rh*Fe* indicate that Ru and Rh are soluble in Fe for small concentrations up to several at.%.[21] As the Ru and Rh concentrations of our sample were 0.1 at.%, f is expected to be identical for Ru and Rh. It is, however, not obvious *a priori* whether the solubility of the precursors, i.e., Cd, Ag, and Pd in the present case, is the more relevant quantity for the implantation behavior, as the sample was not annealed after the irradiation (to save time because of the short half-life of $^{99}Rh^m$). In recoil-implantation experiments with Cd and Ag isotopes,[22,23] high full-field fractions were obtained. If f remains constant in the decay chain, similar fractions are expected for Ru and Rh from this point of view, too. Although the solubility of Pd in Fe seems to be much worse than the solubility of Ru and Rh,[21] we think that this does not play an essential role because of the omitted annealing.

1. ^{97}Ru

The A_2 coefficient for the 215 keV transition is with the known $E2/M1$ multipole mixing ratio $\delta = +0.27(2)$ (Ref. 24) expected to be $A_2 = 0.47(2)$, with which $f(\mathrm{Ru}) = 0.98^{+0.02}_{-0.06}$ is obtained.

2. $^{101}Rh^m$

The A_2 coefficient for the 307 keV transition is with the known $E2/M1$ multipole mixing ratio $\delta = -0.10(5)$ (Ref. 15) expected to be $A_2 = 0.47(8)$, with which $f(\mathrm{Rh}) = 0.98^{+0.02}_{-0.13}$ is obtained.

These data are consistent with the above arguments. Thus we will use the average value $f = 0.98^{+0.02}_{-0.05}$ for the interpretation of the $^{99}Rh^m$ anisotropies. In this way the following $E2/M1$ multipole mixing ratios are determined:

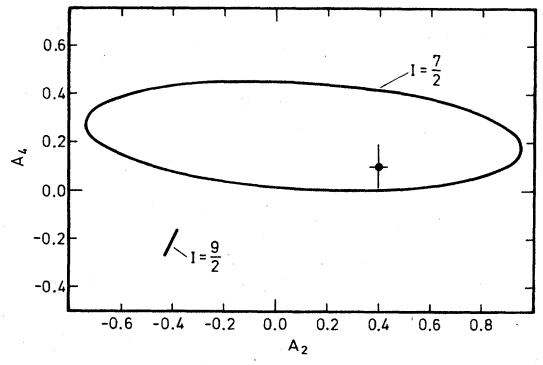

FIG. 11. A_2-A_4 plot for the 1261 keV transition with the assumption of $I=\frac{7}{2}$ and $\frac{9}{2}$ for the 1261 keV level in ^{99}Ru. The degeneracy of the $\frac{9}{2}$ ellipse to a straight line is due to the fact that the tensor rank mixing ratio δ of the $\frac{9}{2} \rightarrow \frac{9}{2}$ β decay enters only quadratically and the following γ transition has pure $E2$ multipolarity.

341 keV: $\delta = -0.05(1)$;

1261 keV: $\delta = -0.07(3)$.

In addition, the spin of the 1261 keV level of ^{99}Ru is uniquely determined to be $\frac{7}{2}$. This can be seen from Fig. 11, where the A_2-A_4 ellipses are plotted for $I(1261) = \frac{7}{2}$ and $\frac{9}{2}$. The measured positive A_2 coefficient definitely rules out $I = \frac{9}{2}$.

D. Magnetic moments

With the hyperfine field $B_{\mathrm{HF}}(\mathrm{Rh}Fe) = -556.6(1.2)$ kG the g factors and magnetic moments of $^{99}Rh^m$ and $^{101}Rh^m$ are deduced to be

$^{99}Rh^m$: $|g| = 1.2595(27)$, $|\mu| = 5.668(12)\ \mu_N$,

$^{101}Rh^m$: $|g| = 1.2167(26)$, $|\mu| = 5.475(12)\ \mu_N$.

Within the present accuracy of the hyperfine field of 0.2%, the hyperfine anomalies between the $\frac{9}{2}^+$ and $\frac{7}{2}^+$ states can be neglected, as the main contributions to the magnetic moments of the $\frac{7}{2}^+$ states arises from the $\frac{9}{2}^+$ proton. Estimates of the hyperfine anomalies in the framework of different models give values between 10^{-5} and, with worst-case assumptions, 10^{-3}. All g factors and magnetic moments known in Rh isotopes from NMR-ON measurements are listed in Table V. The trend is illustrated in Fig. 12. The decrease of the $\frac{9}{2}^+$ g factors from $A=99$ to 101 and of the $\frac{7}{2}^+$ g factors from $A=103$ to 105 can be explained as the core polarization effect of the two additional neutrons. The larger g factors of the $\frac{7}{2}^+$ states in comparison to the $\frac{9}{2}^+$ states prove uniquely that the $\frac{7}{2}^+$ states cannot be described by a three-quasiparticle $|(\pi g_{9/2})^3\rangle_{7/2^+}$ intruder state configuration as adopted up to now, as for this case $g(\frac{7}{2}^+) = g(\frac{9}{2}^+)$ would have been expected in the most simple model. According to theoretical predictions of Kuriyama *et al.*[25] in a more sophisticated model, even $g(\frac{7}{2}^+) < g(\frac{9}{2}^+)$ would have been expected. It should be pointed out here that the trend of g factors illustrated in Fig. 12 is independent of the hyperfine field, as all data result from NMR-ON measurements in Fe, within an accuracy of $\lesssim 10^{-3}$, which is given by the hyperfine anomaly estimated with worst-case assumptions.

Another model which has been proposed for the explanation of $I-1$ states is the weak coupling model, in which these states can be described by a $|2^+ \otimes \pi g_{9/2}\rangle_{7/2^+}$

TABLE V. g factors and magnetic moments of Rh isotopes derived from the hyperfine splitting frequencies of Table III with a hyperfine field $B_{\mathrm{HF}}(\mathrm{Rh}Fe) = -556.6(1.2)$ kG.

Isotope	I^π	$\lvert g \rvert$	μ (μ_N)
$^{99}Rh^m$	$\frac{9}{2}^+$	1.2595(27)	5.668(12)
$^{101}Rh^m$	$\frac{9}{2}^+$	1.2167(26)	5.475(12)
$^{103}Rh^m$	$\frac{7}{2}^+$	1.2971(30)	4.540(11)
^{105}Rh	$\frac{7}{2}^+$	1.2719(27)	4.452(10)

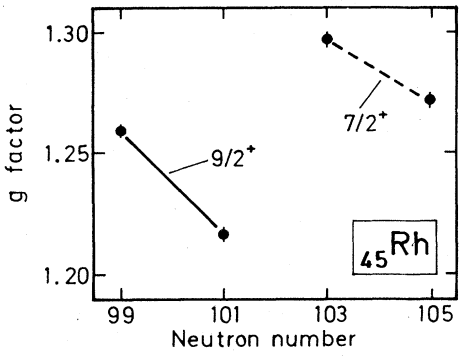

FIG. 12. Trend of the nuclear g factors of $\frac{9}{2}^+$ and $\frac{7}{2}^+$ states in odd Rh isotopes. Note that all data result from NMR-ON measurements in Fe, which means that the accuracy of the relative trend is limited only by the unknown hyperfine anomaly, which is with worst-case assumptions estimated to be $\lesssim 10^{-3}$. The larger g factors of the $\frac{7}{2}^+$ states contradict the assignment of a three-quasiparticle $|(\pi g_{9/2})^3\rangle_{7/2^+}$ intruder state configuration as adopted up to now.

configuration. The g factor for such a configuration is, according to the Lande formula, given by

$$g(\tfrac{7}{2}^+)=\tfrac{23}{21}g_{9/2^+}-\tfrac{2}{21}g_{2^+} . \quad (5)$$

Taking now $g(\frac{9}{2}^+)=1.2167(26)$ ($^{101}\mathrm{Rh}^m$) and $g(2^+)=0.4(1)$, Eq. (5) yields $g(\frac{7}{2}^+)=1.294(10)$. The excellent agreement with $g(^{103}\mathrm{Rh}^m;\ \frac{7}{2}^+)=1.2971(30)$ may be somewhat accidental. In our opinion it is more important that an increase of $g(\frac{7}{2}^+)$ in comparison to $g(\frac{9}{2}^+)$ is predicted, which is actually observed. Thus new theoretical approaches seem to be necessary for the correct interpretation of the $I-1$ states in the mass region $A\sim 100$.

With the hyperfine field $B_{\mathrm{HF}}(\mathrm{Ru}Fe)=-489.6(4.0)$ kG (for the derivation see Ref. 26) the g factor and magnetic moment of the $\nu d_{5/2^+}$ ground state of ^{97}Ru are from the zero-field NMR-ON resonance frequency of 117.58(2) MHz (Sec. IV A) determined to be

$$^{97}\mathrm{Ru}(\tfrac{5}{2}^+):\ |g|=0.315(3),\ |\mu|=0.788(6)\,\mu_{\mathrm{N}} .$$

This result is in good agreement with the less precise values $|g|=0.306(8)$ (Ref. 11) and 0.29(2) (Ref. 26). It fits well into the systematics of $\nu d_{5/2^+}$ g factors in this mass region, as can be seen in the detailed discussions of $\nu d_{5/2^+}$ g factors in Refs. 11 and 26.

Note added in proof. Meanwhile we have received a preprint of K. Nishimura, S. Ohya, and N. Mutsuro (to be published in Nucl. Phys.) who obtained hyperfine splittings in good agreement with our results.

ACKNOWLEDGMENTS

We are indebted to Professor H.-J. Körner for his interest and support of this work. We also wish to thank Dr. P. Maier-Komor and E. Kellner for the preparation of the ^{102}Pd and Fe foils, and Dr. H. Schweickert and K. Assmus for the alpha irradiations at the cyclotron in Karlsruhe. We also acknowledge discussions with K.-H. Ebeling and experimental help by E. Smolic and J. Hesol. This work was supported by the Bundesministerium für Forschung und Technologie, Bonn, and, partly by the Kernforschungszentrum Karlsruhe and the Walther Meissner Institut für Tieftemperaturforschung, Garching.

[1] *Table of Isotopes,* 7th ed., edited by C. M. Lederer and V. S. Shirley (Wiley, New York, 1978).
[2] L. S. Kisslinger, Nucl. Phys. **78**, 341 (1966).
[3] A. I. Sherwood and A. Goswami, Nucl. Phys. **89**, 465 (1966).
[4] H. Kempter and E. Klein, Z. Phys. A **281**, 341 (1977).
[5] E. Hagn, J. Wese, and G. Eska, Phys. Rev. C **23**, 2683 (1981).
[6] S. R. de Groot, H. A. Tolhoek, and W. J. Huiskamp, in *Alpha, Beta, and Gamma Ray Spectroscopy,* edited by K. Siegbahn (North-Holland, Amsterdam, 1968), Vol. 2, p. 1199.
[7] T. Yamazaki, Nucl. Data Sect. A **3**, 1 (1967).
[8] E. Matthias and R. J. Holliday, Phys. Rev. Lett. **17**, 897 (1966).
[9] E. Hagn, P. Kienle, and G. Eska, in *Proceedings of the International Conference on Hyperfine Interactions Studied in Nuclear Reactions and Decay,* Uppsala, Schweden, 1974, edited by E. Karlsson and R. Wäppling (Upplands Grafiska AB, Uppsala, 1974), p. 122.
[10] E. Hagn, K. Leuthold, E. Zech, and H. Ernst, Z. Phys. **295**, 385 (1980).
[11] K. Leuthold, E. Hagn, H. Ernst, and E. Zech, Phys. Rev. C **21**, 2581 (1980).
[12] E. Hagn, E. Zech, and G. Eska, Phys. Rev. C **23**, 2252 (1981).
[13] P. C. Riedi and E. Hagn, Phys. Rev. B **30**, 5680 (1984).
[14] E. Hagn, E. Zech, and G. Eska, J. Phys. F **12**, 1475 (1982).
[15] G. Kaindl, F. Bacon, H.-E. Mahnke, and D. A. Shirley, Phys. Rev. C **8**, 1074 (1973).
[16] E. Matthias, D. A. Shirley, N. Edelstein, H. J. Körner, and B. A. Olsen, in *Hyperfine Structure and Nuclear Radiations,* edited by E. Matthias and D. A. Shirley (North-Holland, Amsterdam, 1968), p. 878.
[17] J. Eisinger and V. Jaccarino, Rev. Mod. Phys. **30**, 528 (1958).
[18] P. A. Moskowitz and M. Lombardi, Phys. Lett. **46B**, 334 (1973).
[19] T. Fujita and A. Arima, Nucl. Phys. **A254**, 513 (1975).
[20] E. Hagn and G. Eska, in *Proceedings of the International Conference on Hyperfine Interactions Studied in Nuclear Reactions and Decay,* Uppsala, Schweden, 1974, edited by E. Karlsson and R. Wäppling (Upplands Grafiska AB, Uppsala, 1974), p. 148.
[21] M. Hansen, *Constitution of Binary Alloys* (McGraw-Hill, New York, 1958), p. 696ff.
[22] R. Eder, E. Hagn, and E. Zech, Phys. Rev. C **30**, 676 (1984).
[23] R. Eder, E. Hagn, and E. Zech, Phys. Rev. C **31**, 190 (1985).
[24] K. S. Krane, At. Data Nucl. Data Tables **19**, 363 (1977).
[25] A. Kuriyama, T. Marumori, and K. Matsuyanagi, Prog. Theor. Phys. **51**, 779 (1974).
[26] E. Hagn, J. Wese, and G. Eska, Z. Phys. A **299**, 353 (1981).